High-pressure structural parameters of the superconductors CeMIn$_5$ and PuMGa$_5$ (M=Co,Rh)

P. S. Normile, S. Heathman, M. Idiri, P. Boulet, J. Rebizant, F. Wastin, and G. H. Lander
European Commission, JRC, Institute for Transuranium Elements, Postfach 2340, D-76125 Karlsruhe, Germany

T. Le Bihan*
European Synchrotron Radiation Facility, Boîte Postale 220, F-38043 Grenoble, France

A. Lindbaum
Vienna University of Technology, Institute for Solid State Physics, Wiedner Hauptstrasse 8-10/138, A-1040 Vienna, Austria
(Received 2 August 2005; revised manuscript received 26 September 2005; published 16 November 2005)

High-pressure, angular-dispersive, x-ray diffraction measurements have been performed on "115" superconductors CeMIn$_5$ and PuMGa$_5$ for M=Co and Rh. The principal results are of the pressure-dependence of the ratio of the tetragonal lattice parameters, c/a, in each system, which are presented for the purpose of understanding the role that this parameter plays in controlling the value of the superconducting temperature T_c. In none of the systems investigated does c/a scale linearly with the value of T_c under pressure, suggesting that it is not the main parameter to control T_c. Values of bulk modulus determined from these measurements are also presented.

DOI: 10.1103/PhysRevB.72.184508 PACS number(s): 61.10.Nz, 74.70.Tx, 74.62.Fj

I. INTRODUCTION

Superconductivity in both the Ce and Pu-115 families Ce$M_xM'_{1-x}$In$_5$ (M,M'=Co,Rh,Ir) and Pu$M_xM'_{1-x}$Ga$_5$ (M,M'=Co,Rh) is unconventional.[1–5] Despite typical transition temperatures (T_c) that differ by around an order of magnitude between the two families (0.4–2.3 K and 8–18.5 K for Ce and Pu families, respectively), it is believed that a similar magnetic pairing mechanism occurs in both classes of compound.[4–6] The tetragonal ($P4/mmm$) crystal structures exhibited in both families may be considered as quasi-two-dimensional (2D), comprising alternately stacked [CeIn3] ([PuGa3]) distorted cuboctahedra and [MIn2] ([MGa2]) rectangular parallelepipeds.[7–10] Antiferromagnetic (AF) correlations associated with such quasi-2D structures have been suggested as possible mediators of the superconductivity in both families.[4,6]

Interestingly, for each family, the differences in T_c from compound to compound (under changes in the doping concentrations of the transition metals M and M' from the group Co, Rh, Ir) are found to correlate with the differences in c/a ratio: the plot of T_c versus c/a forms a straight line of positive gradient for each family.[4] Although the total change in c/a across each family is small ($\sim$3 and $\sim$1 parts in 100 for the Ce and Pu cases, respectively), it is believed to constitute a change in dimensionality, with superconductivity enhanced (T_c increased) by a lowering of dimensionality (increase in c/a).[4] Under high-pressure (P), T_c is found to vary in, generally, the same way for each family: with increasing P, T_c exhibits an inverse-parabolic (or "domelike") dependence.[4,11,12] Figure 1 shows $T_c(P)$ for CeCoIn$_5$, CeRhIn$_5$, PuCoGa$_5$, and PuRhGa$_5$ obtained from high-P resistivity studies.[4,12] For the case of CeRhIn$_5$, there are two points to note. First, at ambient pressure CeRhIn$_5$ is an antiferromagnet, and one has to apply high P (at least 1.6 GPa) to achieve the superconducting state.[1,12,13] Secondly, in addition to the main, domelike shape, an additional feature is observed at P=6.5 GPa (peak position), which is believed to be associated with a second superconducting phase, mediated by a more 3D like ("hidden") magnetic phase.[13]

Given the correlation between T_c and c/a at ambient P across each family, the natural postulate to make (as made in Ref. 4) is that, in *any individual system*, c/a acts as a control parameter for tuning superconductivity (i.e., the value of T_c) under high P, such as to account for the $T_c(P)$ behavior. It is thus important to know how c/a varies under P in each system, to elucidate its relationship to $T_c(P)$. In the panels of Fig. 1, secondary y scales appear on the RHS and correspond to the "anticipated" c/a(P) trends, taking c/a to be the *main* parameter for controlling T_c. Each scale is simply the LHS scale transformed using the parameters (gradient and intercept) of the straight line fit to the $T_c(c/a)$ plot of the respective family. The gradient, $dT_c/d(c/a)$, for the Pu-115 family is a factor $\approx$13 larger than that for the Ce-115's [the values are 72 K/(unit change) and 934 K/(unit change) for the Ce and Pu cases, respectively[4]]. This explains the much smaller changes in c/a anticipated for the Pu-115's as compared with the Ce systems.

In this paper we have determined c/a(P) using high-P, angular-dispersive, x-ray diffraction (ADXRD), employing diamond-anvil cells (DACs), and working at room temperature, in four systems: CeCoIn$_5$, CeRhIn$_5$, PuCoGa$_5$, and PuRhGa$_5$. Values of bulk modulus (B_0) and its pressure derivative (B'_0) have also been determined from these measurements, and are presented for all compounds before presenting the $c/a(P)$ trends. Prior to our studies, high-P, ADXRD studies had been carried out by Kumar and collaborators on CeRhIn$_5$ (Ref. 14) and CeMIn$_5$ (M=Co,Ir),[6] and by Méasson and co-workers on CeCoIn$_5$.[15] We compare our results for the Ce-115's to these previous studies. No high-P XRD study had been carried out on a Pu-115 compound prior to our investigations, the obvious difficulties here arising due to the

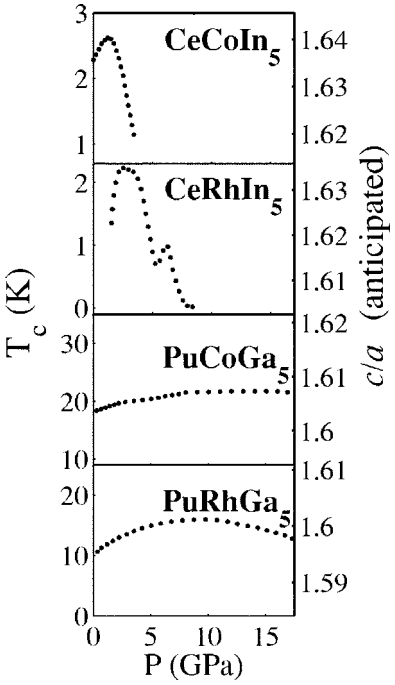

FIG. 1. Experimentally [by high-P resistivity (Refs. 4 and 12)] determined trends in $T_c(P)$ for $CeCoIn_5$, $CeRhIn_5$, $PuCoGa_5$, and $PuRhGa_5$ (only the smooth "guide-to-the-eye" curves (dotted lines) taken through the data points in Refs. 4 and 12 and not the points themselves are shown). The additional y scales on the right-hand side (RHS) of each panel give the "anticipated" c/a ratio, expected if T_c scaled (linearly) with c/a under pressure. The temperature scales [left-hand side (LHS)] are such that the total range of c/a is approximately the same for each panel ($\approx$0.025).

radioactivity of the transuranic material. In collaboration with other laboratories, we have performed high-P XRD experiments on transuranic elements—see, for example, Refs. 16 and 17. The unique methods developed for performing DAC loadings of transuranic materials (reported in these papers) have been employed in this study.

II. EXPERIMENT

Powder samples of CeMIn$_5$ and PuMGa$_5$ (M=Co, Rh) were prepared from starting samples in single-crystal form. Single-crystal CeMIn$_5$ samples were prepared at Los Alamos National Laboratory using the self-flux technique.[7] Single-crystal PuMGa$_5$ samples were prepared at the Institute for Transuranium Elements (ITU), Karlsruhe using a similar (self-flux) method. Powder quantities of $\sim$10 μg, for each compound, were loaded into DACs. For all studies, except that on $PuRhGa_5$, Syassen-Holzapfel type cells (maximum x-ray scattering angle $2\theta_{max} \approx 14°$) were employed. For the $PuRhGa_5$ study, a Le-Toullec type (membrane) cell ($2\theta_{max} \approx 21°$) was used. In all cells, diamond flats were of 300 μm diameter, and inconel gaskets of 150 μm (diameter) hole-size and (indented) thickness 50 μm were used. To avoid the risk of contamination of any exterior part of the DAC by the Pu-containing powder sample, the PuMGa$_5$ powders were combined with a small amount of epoxy resin to form solid

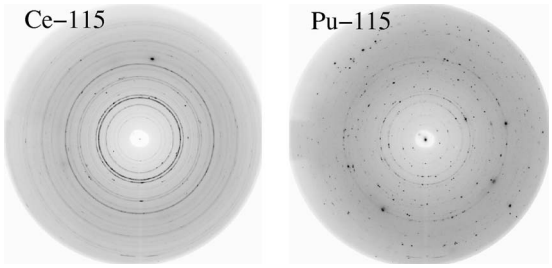

FIG. 2. Examples of (area detector) diffraction patterns for Ce (left image) and Pu (right image) 115 compounds. The Ce data are from the $CeRhIn_5$ run using N_2 (PTM), and the Pu data are from $PuCoGa_5$ (PTM: oil). Both data sets are representative of the typical data from each family (i.e., smooth rings for Ce-115's and spotty rings for Pu-115's), however, the use of a longer x-ray wavelength in $PuRhGa_5$ study implied that a smaller (total) number of rings was collected.

("granular") pieces, which were loaded into the DACs. Silicone oil (hereafter referred to as "oil") was used as the pressure-transmitting medium (PTM) for all compounds. However, in the case of $CeRhIn_5$, a second loading was performed using liquid nitrogen (N_2) as PTM. Pressure was calibrated by the ruby fluorescence method (for each DAC, a single, ruby ball of diameter $<$20 μm was used). Throughout each high-P run, the hole of the gasket was monitored to ensure no "gasket failure" (i.e., a sudden distortion from the circular form of the gasket hole) occurred.

All ADXRD experiments were carried out on the ID30 (undulator) beamline of the European Synchrotron Radiation Facility (ESRF), except for the $PuRhGa_5$ study, which used a rotating anode x-ray generator (Bruker) installed at ITU, Karlsruhe. X-ray wavelength and spot size (at the sample position) were 0.20215 Å and 40×40 μm^2, in the synchrotron measurements, and 0.7094 Å (MoK_{α_1}) and 100×100 μm^2, for the in-house study. Diffraction images, at ID30, were recorded with a MAR345 image plate detector (3450×3450 pixels of dimensions 100×100 μm^2) and, in-house, with a Bruker SMART Apex CCD (1024×1024 pixels of dimensions 61×61 μm^2). DACs were rotated through a sample angle $\Delta\Omega=\pm4°$ while collecting each diffraction image. Examples of diffraction images recorded for Ce and Pu compounds are shown in Fig. 2. We observe that whereas the Debye Scherrer rings are of homogenous intensity in the case of Ce compounds, in the case of Pu-115 samples the rings are severely "spotty." [In $PuRhGa_5$ study, due to the longer x-ray wavelength as compared to the synchrotron studies, only ten ($P4/mmm$) reflections were accessible.] The "spottiness" is due to grain sizes being larger than those for the Ce-115's, given the approximate equivalence of all sample volumes. We attribute the limiting (large) size to a platelike form of the PuMGa$_5$ grains (under a high-resolution, optical microscope, we observed that single crystal pieces of PuMGa$_5$ initially break up, when ground, into platelike crystallites).

The sample to image-plate distance and image-plate non-orthogonality correction were calibrated using powder diffraction data from a Si powder, along with the ESRF software package FIT2D.[18] This software was also used for

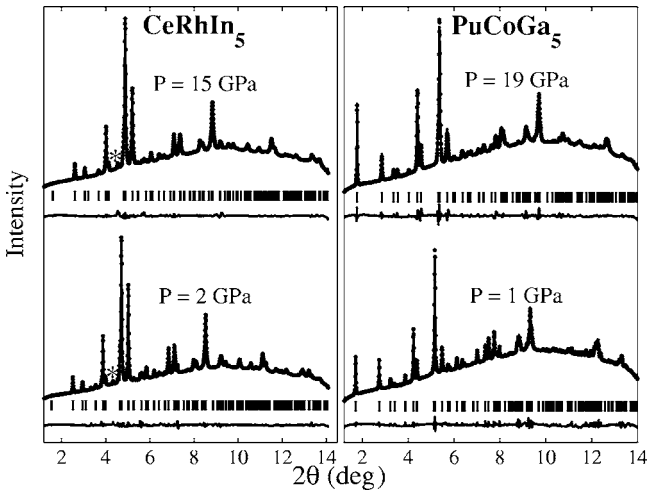

FIG. 3. Examples of diffraction patterns (after integration of area detector data) and fits for Ce (left panel) and Pu (right panel) 115 compounds, at various pressure values. The fits (solid lines through data points) are by profile matching. Reflection positions (vertical bars) and difference curves are also shown; the (001) position, for each pattern, is that of lowest 2θ vertical bar. The weak reflection labeled by an asterisk (Ce-115 patterns) is due to excess In flux. The Ce-115 data is from $CeRhIn_5$ with N_2 as PTM, and the Pu-115 data is from $PuCoGa_5$ (PTM: oil).

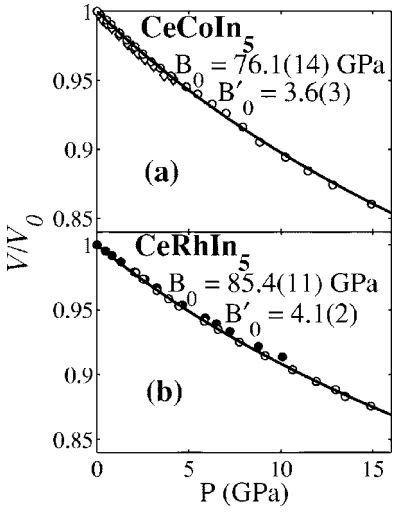

FIG. 4. Normalized unit-cell volume (V/V_0) as a function of pressure for $CeMIn_5$: (a) M=Co and (b) M=Rh. In (a) open points (circles and diamonds) distinguish two runs [ours and one performed by Méasson *et al.* (Ref. 15), respectively] which used the same type of PTM (oil). In (b) open points are for a run with N_2 as PTM, and closed points are with oil. The solid lines are fits to a Birch-Murnaghan equation of state, with the corresponding B_0 and B_0' values given [errors on these values refer to the least significant digit(s)]. Errors on the pressure variable and relative volumes are smaller than the plotting points.

integration of diffraction images (intensity summation around each ring) for all samples investigated, providing a data format suitable for structural refinements. These refinements were carried out by profile matching (otherwise known as Le Bail fitting[19]), using the FULLPROF package.[20] (Note that the spotty diffraction patterns for Pu-115 made Rietveld refinement impossible.) Figure 3 shows examples of the typical fits to diffraction patterns obtained. A notable difference between the patterns for the Ce and Pu compounds is that the intensity of the first Bragg reflection, the (001), is negligible in the case of the Ce-115's. The quality of the fits obtained to the Ce-115 data were, in general, better than those of the Pu for reasons discussed above, concerning powder quality. Bragg (reliability) factors were, in general, ~5% for the Pu work, and for the Ce work, lower still.

The values of the ambient-P, unit-cell volume V_0 were, for the Ce-115 compounds, obtained from diffraction patterns from samples at ambient P. However, due to safety issues relating to the risk of (Pu) contamination, it was not possible to do the same for the Pu-115 powders; the samples had to remain "truly encapsulated" (i.e., gasket holes well sealed by diamond anvils) which implied nonambient P starting conditions [=0.7(1) GPa and 2.5(1) GPa for $PuCoGa_5$ and $PuRhGa_5$, respectively]. The values of V_0 were then "extrapolated" from the $V(P)$ data at low $P(<10$ GPa) by fitting Birch-Murnaghan curves,[22] with V_0 as a fitting parameter and B_0' fixed to a value of 4.

In the analysis of the data for $PuMGa_5$, only, given the spotty rings, an additional lattice parameter refinement of the c axis (only) was made using a single diffraction spot in the (001) ring. The 2θ position of the spot as a function of P was determined by Voigt function fitting to its intensity profile (extracted using the CAKE integration option of FIT2D). This refinement method is similar to that used in a recent, high-P single-crystal diffraction study to recalibrate the ruby pressure scale.[21]

III. RESULTS

A. Bulk compressibilities

The volume compressibility curves for $CeMIn_5$ and $PuMGa_5$ are shown in Figs. 4 and 5, respectively. For $CeCoIn_5$ [Fig. 4(a)] only one run (open circles) was performed in our studies, using oil as PTM, and the second data-set (open diamonds) is from an ESRF (ID30 beam-line) study by Méasson *et al.*,[15] which also used oil as PTM and reached 4.2 GPa. The data overlap demonstrates excellent agreement between the two experiments. For $CeRhIn_5$ [Fig. 4(b)] two runs were performed, one using oil (closed circles) and the other using N_2 (open circles) as PTM. As usual in experiments employing N_2 as PTM, the starting P was relatively high (~2 GPa).

For $PuCoGa_5$ [Fig. 5(a)] an anomaly ("bump") is observed in the volume in the range 10–14 GPa. This is associated to the pressure-induced freezing of the PTM (oil)—see Refs. 23 and 24 for examples of high-P studies where similar effects have been observed. We attribute the preferential presence of this (freezing) anomaly in the experiment on $PuCoGa_5$, as compared to the Ce-115 studies employing the same PTM, to the larger ($PuCoGa_5$) grain sizes and also their platelike form. The presence of the freezing anomaly renders the $PuCoGa_5$ data above 10 GPa to be (quantitatively) unreliable. Given the equivalence of PTM and the form and sizes

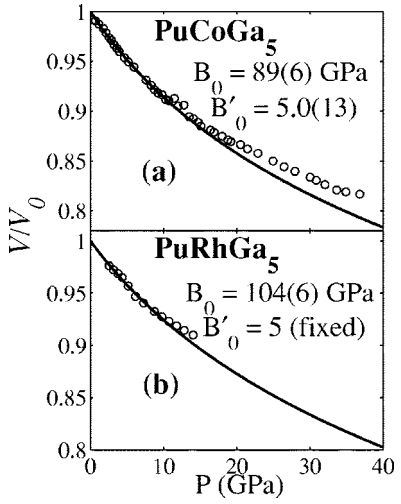

FIG. 5. Normalized unit-cell volume (V/V_0) as a function of pressure for PuMGa$_5$: (a) M=Co and (b) M=Rh. In both (a) and (b), the solid lines are Birch-Murnaghan fits made to the data in the range $P<10$ GPa. Values of B_0 and B_0' [with errors to the least significant digit(s)] corresponding to each fit are given [in (b) B_0' was fixed]. Errors on the pressure variable and relative volume are smaller than the plotting points.

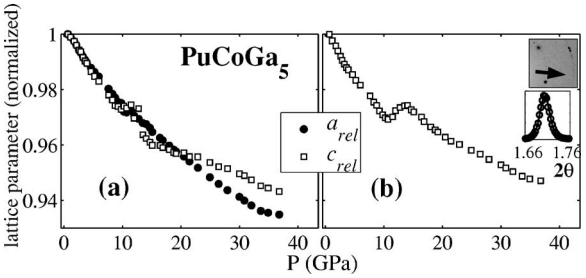

FIG. 6. Normalized lattice parameters a_{rel} and c_{rel} in PuCoGa$_5$ as a function of pressure (the values have been normalized to unity at the starting pressure of 0.7 GPa), showing an anomaly in c in the range 10–14 GPa due to PTM freezing. The values were obtained by (a) an analysis of the entire diffraction pattern and (b) (c lattice parameter only) an analysis of a single diffraction spot. The upper inset in (b) shows the relevant "spot" [from the (001) ring] at 0.7 GPa. Here the arrow points in the direction of increasing 2θ; the spot is located just below this arrow. The lower inset shows the profile of the spot along the 2θ direction, fitted to a Voigt function. Errors on lattice parameters in (a) and (b) are smaller than the plotting points.

of the powder grains in both Pu-115 studies, we assume the PuRhGa$_5$ data [Fig. 5(b)] above 10 GPa to be also unreliable.

The solid lines in Figs. 4 and 5 are fits to a Birch-Murnaghan (BM) form for the equation of state (EOS);[22] the values of B_0 and B_0' for each compound, obtained from each fit, are given in the figures. The value of B_0 obtained for CeCoIn$_5$ is in good agreement with the value of 78.2(18) GPa reported by Kumar *et al.*[6] However, for CeRhIn$_5$ we obtain a B_0 value larger than that of 78.4(20) GPa reported by the same authors.[14] The fit for CeRhIn$_5$ [Fig. 4(a)] takes into account all the points from the N_2 run and (only) the first four points from the oil run. The reason for this is that N_2, in general, provides better hydrostatic conditions than oil. The superior PTM, as well as the reduced scatter in our data compared to those presented in Ref. 14, render our determination of B_0 for CeRhIn$_5$ to be more reliable. The fits for both Pu-115 compounds [Figs. 5(a) and 5(b)] are to the data in the range $P<10$ GPa only, given the unreliability of the data above 10 GPa. This explains the deviation, for $P>10$ GPa, of the data points from the fitted curves in Figs. 5(a) and 5(b). The value of B_0 obtained for PuCoGa$_5$ is in good agreement with the value of 87 GPa determined in recent density functional electronic structure calculations for PuCoGa$_5$.[25]

Notwithstanding the relatively low values for the maximum pressure P_{max} of the data being fitted [$P_{\mathrm{max}}<0.2B_0$ in all cases], the fitted values of B_0', being ~ 4 [Figs. 4 and 5(a)], are reasonable (see, for example, Ref. 26 for typical B_0' values for actinide intermetallics). For PuRhGa$_5$ [Fig. 5(b)] the value of B_0' has been fixed to the value obtained for PuCoGa$_5$ [Fig. 5(a)].

B. Anomaly in c lattice parameter in PuMGa$_5$ associated with freezing of PTM

An inspection of the individual lattice parameters a and c in PuCoGa$_5$ as a function of P reveals that the anomaly in the compressibility curve [Fig. 5(a)] is due to an anomalous behavior in the c lattice parameter, as shown in Fig. 6(a). In the range $10<P<14$ GPa, one observes [Fig. 6(a)] that as the PTM freezes, the c lattice parameter relaxes. That the anomaly is less pronounced in V/V_0 [Fig. 5(a)] is because V depends more strongly on the a parameter ($V\propto a^2$) than the c($V\propto c$), and the former lattice parameter behaves normally as the PTM freezes. A similarly anomalous behavior in the c parameter (for $P\gtrsim 10$ GPa) is found in our study on PuRhGa$_5$.

Whereas the lattice parameters in Fig. 6(a) have been obtained by profile matching of the full diffraction pattern, in Fig. 6(b) the P dependence of the c lattice parameter determined from the position of a single diffraction spot in the (001) ring is shown. The insets of Fig. 6(b) show, respectively, the segment of the image plate diffractogram where the spot is located and the (integrated) intensity profile (of the spot) along 2θ. Other diffraction spots comprising the (001) ring were identified, however, only the spot used remained at a fixed position on the image plate throughout the P range of the experiment. With increasing P, the intensity profile of the spot along 2θ remains a single peak [with a Voigt profile, as in the lower inset of Fig. 6(b)], whereas along the azimuthal direction (i.e., perpendicular to 2θ) the profile, which is initially a single peak, becomes a double peak as the pressure becomes nonhydrostatic (i.e., $P>10$ GPa). The anomaly in the c lattice parameter deduced from this analysis is more pronounced than that observed when analyzing the full diffraction pattern [Fig. 6(a)], indicating that the degree of c parameter relaxation (under the freezing of the PTM) varies between different grains.

C. Trends in c/a

Figure 7(a) shows the trend in c/a we have determined from our measurements on CeRhIn$_5$, and in Fig. 7(b) our results are compared to those of Kumar *et al.*[14] by means of

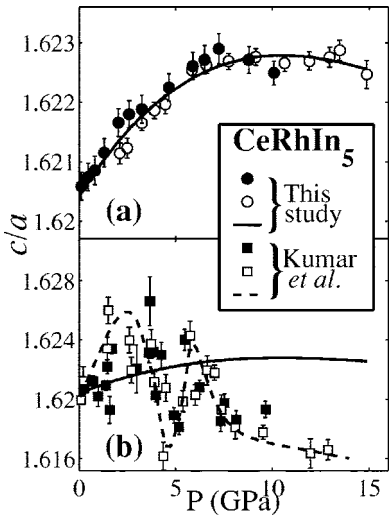

FIG. 7. c/a as a function of pressure in $CeRhIn_5$: (a) from this study (circles) and (b) from the Kumar *et al.* study (Ref. 14) (squares). In each panel, closed and open points distinguish data from runs using different PTMs; for our data, closed are for oil and open for N_2. The solid line (guide-to-the-eye) curve through our data in (a) is reproduced in (b) [where it appears "flatter" due to the $(4\times)$ larger y-scale range of the lower panel]. The dashed line curve in (b) is the trend Kumar *et al.* conclude from their data.

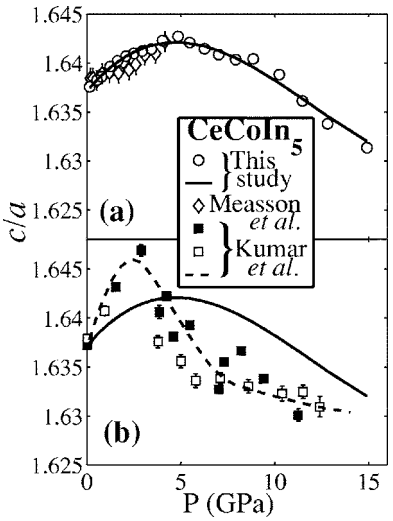

FIG. 8. c/a as a function of pressure in $CeCoIn_5$: (a) from this study (circles) and (b) from the Kumar *et al.* study (Ref. 6) (squares). In (a) the results from a study by Méasson *et al.* (Ref. 15) are also shown (open diamonds; $P<4.2$ GPa). The solid line (guide-to-the-eye) curve through our data in (a) is reproduced in (b) (the sizes of y-scale ranges are identical in the two panels). The dashed line in (b) is the trend Kumar *et al.* conclude from their data.

replotting the curve (solid line) made through our data points. (Note that this curve, as with our data fitting curves in subsequent figures, is simply a polynomial, "guide-to-the-eye" fit.) We obtain excellent agreement between the $c/a(P)$ trends obtained using oil and N_2 [Fig. 7(a)], respectively, as PTM. In the P range 0 to 6 GPa, where the previous study concludes a double peak variation [dashed curve, Fig. 7(b)], we observe c/a to monotonically increase with each pressure increment. The scatter of our data about a smooth curve taken through the points is considerably less than in the case of the Kumar *et al.* study.

Figure 8(a) shows the trend in c/a we have determined for $CeCoIn_5$. As in Fig. 7, the lower panel [Fig. 8(b)] compares our results (solid line) with the results from the study of Kumar *et al.*[6] As in Fig. 4, we plot our data on the same axes as the results of Méasson *et al.*[15] and observe that the agreement is excellent between the two experiments ($P<4.2$ GPa). In Fig. 8(b) we observe "some" qualitative agreement with the Kumar *et al.* study in that, in the range $0<P<15$ GPa, $c/a(P)$ is a single-peak function, with peak position between 2.5 and 5 GPa. As in the case of $CeRhIn_5$, however, our data points are less scattered than for the Kumar *et al.* study.

Figure 9 presents the results for PuMGa$_5$. Considering first the case of M=Co, we observe two distinct trends in c/a: a fall with increasing P up to 10 GPa, followed by a rise with increasing $P>14$ GPa. The points in the region $10<P<14$ GPa vary strongly with each P step, which is due to the relaxation effect in the c parameter [note that we have used lattice parameters determined from the analysis of the full diffraction patterns, Fig. 6(a)]. Given that this effect is an artifact associated with freezing of the PTM, we have not taken into account these points in the curve (solid line) we make through the data points. For $PuRhGa_5$, we observe c/a to fall with increasing P (from the starting P of 2.5 GPa) up to $P\approx 8$ GPa, and then begin to rise. As with the case of $PuCoGa_5$, the curve (solid line) does not take account of the data between 10 and 14 GPa (maximum P reached in the experiment) due to the anomalous c parameter in this P range.

IV. DISCUSSION

The achievement of hydrostatic pressure has been a goal in all our studies. However, for the case of Pu-115, safety

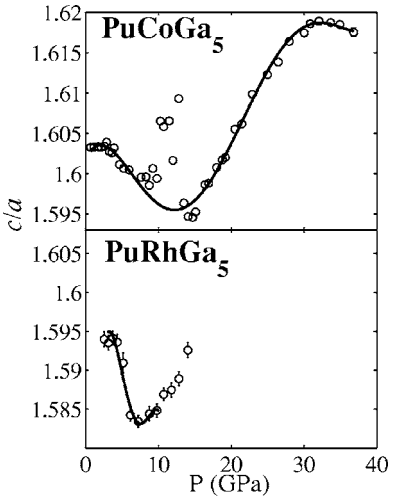

FIG. 9. c/a as a function of pressure in PuMGa$_5$ (M=Co,Rh). The solid line (guide-to-the-eye) curves neglect the points in the range 10 GPa$<P<$14 GPa, for the reason explained in the text.

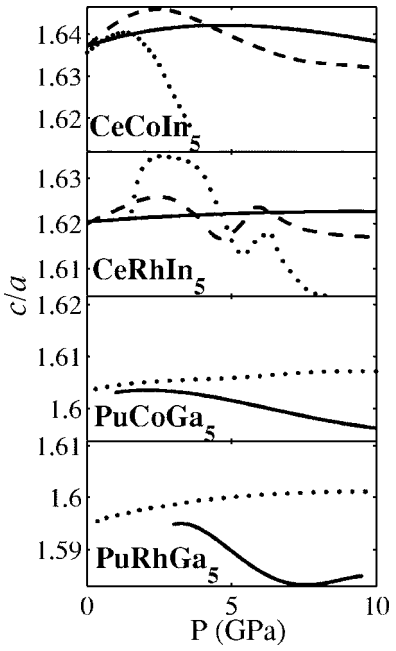

FIG. 10. Summary of results: experimentally determined trends (solid lines) in c/a as a function of pressure for all the compounds investigated in this study compared to the *anticipated* trends from Fig. 1 (dotted lines). For the Ce-115 compounds, the trends in c/a(P) derived experimentally by Kumar *et al.* (Refs. 14 and 6) are also shown (dashed lines).

issues relating to loading transuranic samples in powder form (unfortunately, high-quality polycrystalline samples were not available) limited our studies to the use of an oil-based PTM. The combination of the freezing of the silicone oil and the large crystallite grain size for Pu-115 (revealed by spotty diffraction images—see Fig. 2) has resulted in our determinations of $c/a(P)$ being unreliable in the range $10\ \text{GPa} < P < 14\ \text{GPa}$. Indeed, the upturn in c/a for $P > 14$ GPa in $PuCoGa_5$ (Fig. 9) may not occur in a situation in which no freezing of the PTM (and resulting relaxation of the c lattice parameter) occurs. Thus, we may say that our determinations of $c/a(P)$ for Pu-115 are only (strictly) reliable below 10 GPa.

Our experiments on Ce-115 have not suffered due to the freezing of silicone oil, and we attribute this to a "finer" powder grain size (concomitant with smooth diffraction rings—see Fig. 2) as compared to the Pu-115 powders. In particular, an experiment made on $CeRhIn_5$ using N_2 as PTM has shown an identical trend in $c/a(P)$ as the experiment employing oil [Fig. 7(a)]. Comparisons with previous studies on Ce-115 (Kumar *et al.*[6,14] and Méasson *et al.*[15]) imply the necessity of hydrostatic pressure to achieve the required sensitivity in the determination of c/a (see Fig. 1), i.e., a sensitivity of less than 1 part in 100 in the relative change in c/a under P. We may add that in spite of the problems incurred with Pu-115, we still appear to achieve a sensitivity in the determination of c/a below 10 GPa higher than in the experiments on $CeRhIn_5$ performed by Kumar *et al.*[14] [Fig. 7(b)].

Figure 10 gives a comparison of our $c/a(P)$ trends [only the curves from Figs. 7(a), 8(a), and 9, and not the data points] with the trends which would be expected if $T_c(P)$ scaled linearly with c/a under high-P, i.e., the "anticipated c/a" (Fig. 1). We plot the results for $P < 10$ GPa only, for two reasons. First, for the two Ce-115 compounds, superconductivity does not exist above 10 GPa. Secondly, for the Pu-115's, as stated above, our determination of $c/a(P)$ is only (strictly) reliable below 10 GPa. None of our measured trends shown in Fig. 10 are found to agree with expectation. We present also in Fig. 10 the $c/a(P)$ trends determined by the work of Kumar *et al.*[6,14] As with our trends, these previously determined trends do not agree with expectation either.

The small changes in c/a occurring under high-P in any individual system from our experiments suggest that c/a is not the main driving parameter for controlling the value of T_c under high P in these systems (Fig. 10). The remarkable correlation between T_c and c/a at ambient P across each 115 family [reported in Ref. 4 for $CeM_xM'_{1-x}In_5$ (M,M' =Co,Rh,Ir) and $PuM_xM'_{1-x}Ga_5$ (M,M'=Co,Rh)], thus, does not appear to be related to the $T_c(P)$ behavior exhibited in these systems in as simple a way as initially postulated. What is clear is that across the solid solutions, changing the relative concentrations of transition metals M and M' has two effects: (i) it modifies (slightly) the crystal structure, changing the values of lattice parameters a and c, and their ratio c/a and (ii) it alters the value of T_c. The former effect is certainly related to a change in radius of the M atom down the d group (Co to Ir). The change in T_c, however, may also be a consequence of a change in the d bandwidth [between the $3d$ (Co), $4d$ (Rh), and $5d$ (Ir) bands], in addition to the small changes (~ 3 and ~ 1 parts in 100 for the Ce and Pu families, respectively, see Fig. 3 from Ref. 4) in c/a. Recent work on $PuCoGa_5$,[27] for example, has investigated the effect of doping the Co site with a d element from a different group of the periodic table (i.e., $PuCo_xFe_{1-x}Ga_5$ and $PuCo_xNi_{1-x}Ga_5$), and observes that both families (in particular $PuCo_xFe_{1-x}Ga_5$) exhibit gradients $dT_c/d(c/a)$, that differ from that for $PuCo_xRh_{1-x}Ga_5$. The effect that pressure has on the hybridization between the Ce (Pu) atoms and the M and In (Ga) atoms (of the form[6] fd and fp, respectively), as well as on other structural parameters [for example,[28] the parameter $(2zc-a)/a$], may also relate to why the $T_c(c/a)$ correlation and $T_c(P)$ behavior in Ce (Pu) 115's may not be so simply connected as initially postulated.[4]

V. CONCLUSIONS

We have presented results from high-P ADXRD studies on $CeCoIn_5$ and $CeRhIn_5$ (both up to 15 GPa), $PuCoGa_5$ (up to 37 GPa), and $PuRhGa_5$ (up to 14 GPa). The bulk compressibility parameters (B_0 and B'_0) are summarized in Table I, together with the most reliable measurements of lattice parameters (at ambient P) found in the literature. Our value of B_0 for $PuCoGa_5$ is in good agreement with theory,[25] which predicts $B_0 = 87$ GPa. (We are unaware of any calculations of B_0 in the literature for $CeCoIn_5$, $CeRhIn_5$, or $PuRhGa_5$.)

In all compounds investigated, the experimentally determined changes in the c/a ratio do not agree with an expectation that this ratio acts as the main tuning parameter for controlling the value of T_c under pressure. For $CeRhIn_5$, our

TABLE I. Experimentally determined values of lattice parameters a_0 and c_0 [these are ambient pressure values (Refs. 7, 8, and 10)] and bulk moduli B_0 and its pressure derivative B_0' (from Birch-Murnaghan equation of state fits to the diffraction data from this study) for certain Ce and Pu-115 compounds. For the Ce-115's, we show also, in italics, the values of B_0 and B_0' determined in the experiments of Kumar *et al.* (Refs. 6 and 14) For $PuRhGa_5$, our value of B_0' has been fixed due to limited diffraction data at low pressure ($P<10$ GPa) collected for this sample. References for the lattice parameter data are as follows: Ref. 7 ($CeCoIn_5$), Ref. 8 ($CeRhIn_5$), and Ref. 10 ($PuCoGa_5$ and $PuRhGa_5$). Errors on all values refer to least significant digit(s).

Compound	a_0 (Å)	c_0 (Å)	B_0 (GPa)	B_0'
$CeCoIn_5$	4.61292(9)	7.5513(2)	76.1(14), *78.2(18)*	3.6(3), *3.9(4)*
$CeRhIn_5$	4.652(1)	7.542(1)	85.4(11), *78.4(20)*	4.1(2), *5.6(6)*
$PuCoGa_5$	4.2354(1)	6.7939(2)	89(6)	5.0(13)
$PuRhGa_5$	4.3012(1)	6.8569(2)	104(6)	5.0 (fixed)

values of $c/a(P)$ are considerably less scattered than in a study by Kumar *et al.*,[14] demonstrating that c/a increases monotonically with increasing P from 0 to 6 GPa, rather than exhibiting the double-peak behavior expected. For $CeCoIn_5$, $c/a(P)$ is a single-peak function, as expected, but neither the position of the maximum nor the peak amplitude agree with expectation. For both $PuCoGa_5$ and $PuRhGa_5$ we observe c/a to fall with increasing P up to $P\approx 8$ GPa, rather than to rise to a maximum.[4]

In the case of $PuMGa_5$, the determination of both $c/a(P)$ and the bulk-compressibility parameters have been limited to the pressure range $P<10$ GPa due to effects associated with the freezing of oil (PTM). Future work (on $PuMGa_5$) employing a better PTM, e.g., such as N_2, should, for safety issues involved in performing DAC loadings of transuranium materials, study samples in single-crystal rather than powder form (high-quality polycrystalline Pu-115 samples are not available). Indeed, the use of single crystals in high-P XRD is proving pertinent to improved compressibility data due to improved precision in (relative) lattice parameter (as a function of P) determination as compared to a powder method.[21]

ACKNOWLEDGMENTS

We thank E. D. Bauer and J. L. Sarrao of Los Alamos National Laboratory for providing the single-crystal Ce-115 samples. The high purity Pu metal required for the fabrication of the Pu-115 compounds was made available through a loan agreement between Lawrence Livermore National Laboratory and ITU, in the frame of a collaboration involving LLNL, Los Alamos National Laboratory, and the U.S. DOE. P.S.N. and M.I. acknowledge the European Commission for support in the frame of the Training and Mobility of Researchers programme.

*Present address: CEA Valduc, DRMN/SEMP/LECP, F-21120 Is-sur-Tille, France.

[1] H. Hegger, C. Petrovic, E. G. Moshopoulou, M. F. Hundley, J. L. Sarrao, Z. Fisk, and J. D. Thompson, Phys. Rev. Lett. **84**, 4986 (2000).
[2] C. Petrovic, P. G. Pagliuso, M. F. Hundley, R. Movshovich, J. L. Sarrao, J. D. Thompson, Z. Fisk, and P. Monthoux, J. Phys.: Condens. Matter **13**, L337 (2001).
[3] P. G. Pagliuso, C. Petrovic, R. Movshovich, D. Hall, M. F. Hundley, J. L. Sarrao, J. D. Thompson, and Z. Fisk, Phys. Rev. B **64**, 100503(R) (2001).
[4] E. D. Bauer *et al.*, Phys. Rev. Lett. **93**, 147005 (2004).
[5] N. J. Curro, T. Caldwell, E. D. Bauer, L. A. Morales, M. J. Graf, Y. Bang, A. V. Balatsky, J. D. Thompson, and J. L. Sarrao, Nature (London) **434**, 622 (2005).
[6] R. S. Kumar, A. L. Cornelius, and J. L. Sarrao, Phys. Rev. B **70**, 214526 (2004).
[7] E. G. Moshopoulou, Z. Fisk, J. L. Sarrao, and J. D. Thompson, J. Solid State Chem. **158**, 25 (2001).
[8] E. Moshopoulou, J. L. Sarrao, P. G. Pagliuso, N. O. Moreno, J. D. Thompson, Z. Fisk, and R. M. Ibberson, Appl. Phys. A: Mater. Sci. Process. **74**, S895 (2002).
[9] J. L. Sarrao, L. A. Morales, J. D. Thompson, B. L. Scott, G. R. Stewart, F. Wastin, J. Rebizant, P. Boulet, E. Colineau, and G. H. Lander, Nature (London) **420**, 297 (2002).
[10] F. Wastin, P. Boulet, J. Rebizant, E. Colineau, and G. H. Lander, J. Phys.: Condens. Matter **15**, S2279 (2003).
[11] J.-C. Griveau, C. Pfleiderer, P. Boulet, J. Rebizant, and F. Wastin, J. Magn. Magn. Mater. **272**, 154 (2004).
[12] T. Muramatsu, N. Tateiwa, T. Kobayashi, A. Shimizu, K. Amaya, D. Aoki, H. Shishido, Y. Haga, and Y. Onuki, J. Phys. Soc. Jpn. **70**, 3362 (2001).
[13] M. Nicklas, V. A. Sidorov, H. A. Borges, P. G. Pagliuso, J. L. Sarrao, and J. D. Thompson, Phys. Rev. B **70**, 020505(R) (2004).
[14] R. S. Kumar, H. Kohlmann, B. E. Light, A. L. Cornelius, V. Raghavan, T. W. Darling, and J. L. Sarrao, Phys. Rev. B **69**, 014515 (2003).
[15] M.-A. Méasson , T. Le Bihan, and D. Braithwaite (unpublished).
[16] S. Heathman, R. G. Haire, T. Le Bihan, A. Lindbaum, K. Litfin, Y. Méresse, and H. Libotte, Phys. Rev. Lett. **85**, 2961 (2000).
[17] S. Heathman, R. G. Haire, T. Le Bihan, A. Lindbaum, M. Idiri, P. Normile, S. Li, R. Ahuja, B. Johansson, and G. H. Lander, Science **309**, 101 (2005).
[18] A. P. Hammersley, S. O. Svensson, M. Hanfland, A. N. Fitch, and D. Haüsermann, High Press. Res. **14**, 235 (1996).
[19] A. Le Bail, H. Duroy, and J. L. Fourquet, Mater. Res. Bull. **23**, 447 (1988).
[20] J. Rodriguez-Carvajal, Physica B **192**, 55 (1993).
[21] A. Dewaele, P. Loubeyre, and M. Mezouar, Phys. Rev. B **70**, 094112 (2004).
[22] F. Birch, Phys. Rev. **71**, 809 (1947).
[23] T. Le Bihan, S. Heathman, M. Idiri, G. H. Lander, J. M. Wills, A. C. Lawson, and A. Lindbaum, Phys. Rev. B **67**, 134102 (2003).

[24] U. Ponkratz, F. Porsch, G. Wortmann, and W. Holzapfel, J. Alloys Compd. **359**, 99 (2003).
[25] P. Söderlind, Phys. Rev. B **70**, 094515 (2004).
[26] U. Benedict and W. B. Holzapfel, *Handbook on the Physics and Chemistry of Rare-Earths* (Elsevier Science, Netherlands, 1993), Vol. 17, pp. 245–300.
[27] P. Boulet, E. Colineau, F. Wastin, J. Rebizant, P. Javorský, G. H. Lander, and J. D. Thompson, Phys. Rev. B **72**, 104508 (2005).
[28] J. D. Thompson, M. Nicklas, V. A. Sidorov, E. D. Bauer, R. Movshovich, N. J. Curro, and J. L. Sarrao, J. Alloys Compd. (to be published).